Numerical Analysis of the Transient Behavior of the Non-Equilibrium Quantum Liouville Equation

Lukas Schulz and Dirk Schulz

***Abstract*—The numerical analysis of transient quantum effects in heterostructure devices with conventional numerical methods tends to pose problems. To overcome these limitations, a novel numerical scheme for the transient non-equilibrium solution of the quantum Liouville equation utilizing a finite volume discretization technique is proposed. Additionally, the solution with regard to the stationary regime, which can serve as a reference solution, is inherently included within the discretization scheme for the transient regime. Resulting in a highly oscillating interference pattern of the statistical density matrix as well in the stationary as in the transient regime, the reflecting nature of the conventional boundary conditions can be an additional source of error. Avoiding these non-physical reflections, the concept of a complex absorbing potential used for the Schrödinger equation is utilized to redefine the drift operator in order to render open boundary conditions for quantum transport equations. Furthermore, the method allows the application of the commonly used concept of inflow boundary conditions.**

***Index Terms*—Quantum Liouville equation, drift operator, numerical schemes, quantum transport, resonant tunneling devices, complex absorbing potential.**

I. Introduction

TRANSIENT effects in todays quantum devices form the basis for applications in ultra fast electronics and photonics. Unfortunately, conventional models for the numerical analysis of the transient behavior of the device under investigation are associated with problems.

The majority of the common models allowing a detailed analysis of the carrier transport mechanism is either based on the non-equilibrium Green's function (NEGF) approach [1], [2] or the numerical solution of the Wigner Transport Equation (WTE) [3]–[8]. Beyond, methods utilizing concepts of quantum field theory can be applied for a numerical solution of the statistical density matrix [9], [10]. Here, a concept suitable for the analysis of engineering applications is addressed. The numerical solution of the NEGF formalism [1], [2] is fundamentally addressed by the inversion of the Hamilton-Operator of the system. As a consequence, the application of the NEGF formalism exhibits an enormous complexity with regard to computational costs. The conventional numerical solution methods for the WTE are either based on a finite difference scheme [3]–[5] or a Monte Carlo integration technique [6]. The Monte Carlo solution of the WTE is limitated regarding the computational costs of the algorithm. Hence, from the engineering point of view the application of a finite difference scheme is preferable as it allows an efficient solution of the WTE. The conventional numerical solution is based on the application of an upwind difference scheme (UDS) [3]–[5]. Unfortunately, the UDS approximation is found to be deficient [7], when a spatially varying potential distribution is considered as discussed in the following. To start with, the separation of forward and backward traveling waves within the discretized diffusion operator leads to an inadequate inclusion of coherent effects [7]. Indeed, this aspect is reflected in the overestimation of the diffusion effect [11]. Furthermore, the non-local kinetic operator is not interacting with the boundary conditions [12]. Consequently, non-physical results, i.e., negative carrier distributions, can be obtained [7], [12].

To conclude, the models are either to costly with regard to computational resources or can be limitated in the reliability of the results. Therefore, conventional numerical schemes are only conditionally applicable.

Recently, two schemes have been presented [7], [13], which overcome the drawbacks of the conventional finite difference scheme, inherently including an adequate description of coherent effects. Especially, in [13] the proposed method has been compared with results stemming from the quantum transmitting boundary method (QTBM) [14] for the self-consistent non-equilibrium case. The proposed approach in [13] shows an excellent agreement with the QTBM as a reference solution. Note, that the QTBM is a numerical equivalent of the NEGF formalism [15], [16].

Following the concept of [7], [13], the solution procedures utilize the formulation of a spatially dependent exponential operator as a similarity neglecting the transient behavior. Therefore, these approaches [7], [13] are limited to the stationary regime.

For this reason, we present a novel approach based on the Quantum Liouville Equation (QLE) that preserves the characteristics of [7], [13] and enables the transient analysis. Moreover, the stationary solution is inherently included in the proposed approach being equivalent with the approach in [13] when a Taylor approximation is applied onto the exponential operator. To address the concept of self-energy terms, we take up the idea of a complex absorbing potential (CAP), that until

Manuscript received April 23, 2018; revised July 18, 2018; accepted August 31, 2018. Date of publication September 13, 2018; date of current version November 8, 2018. This work was supported by the German Research Funding Association Deutsche Forschungsgemeinschaft under Grant SCHU 1016/8-1. The review of this paper was arranged by S. Pontarelli. *(Corresponding author: Lukas Schulz.)*

The authors are with the Chair for High Frequency Techniques, Technische Universität Dortmund, Dortmund 44227, Germany (e-mail: lukas.schulz@tu-dortmund.de; dirk2.schulz@tu-dortmund.de).

Digital Object Identifier 10.1109/TNANO.2018.2868972

today is only applied onto the Schrödinger equation [17], [18]. For an adequate inclusion in the proposed approach, the drift operator has to be redefined.

The contribution is organized as follows. In Section II, the basics regarding quantum transport in the real space presentation is introduced. Then, the approximation procedure of the QLE utilizing a finite volume discretization technique is described in Section III including the boundary treatment, in which the drift operator is defined retaining the characteristics of CAP. A comparison with a transient solution based on the QTBM [19] is preferable. Unfortunately, this approach inherently suffers from singularity issues when a ballistic regime is considered. Therefore, the proposed approach is applied onto a standard resonant tunneling diode and subsequently compared with the results obtained from the conventional numerical solution of the WTE followed by a summary and conclusion in Section V.

II. Nanoscale Transport Based on the Quantum Liouville Equation

A. Theory

Starting with major relations, the fundamentals are introduced briefly. The transient behavior of the statistical density matrix ρ is determined by the QLE according to

$$\partial_t \rho = \mathcal{L}\rho, \tag{1}$$

where $\mathcal{L}$ represents the Liouville Operator. For the exemplary analysis of quantum wells with the variable x being the growth direction, it is sufficient to consider a one-dimensional effective mass Hamiltonian $\mathcal{H}$ given by

$$\mathcal{H} = -\frac{\hbar^2}{2m}\partial_x^2 + eV(x) + \frac{\hbar^2}{2m}k_{||}^2. \tag{2}$$

The constant e represents the elementary charge of an electron and $\hbar$ is the reduced Planck's constant. The lateral wavevector $k_{||}$ is related to the lateral y- and z-direction based on the periodicity of the lattice. The real part of the electrostatic potential $\Re\{V\}$ includes both the conduction band- and the self-consistent Hartree-Fock-potential. The imaginary part of potential $\Im\{V\}$ is related to the complex absorbing potential, which is discussed in Section III. Furthermore, the effective mass distribution m is assumed to be constant for simplicity. Of course, the proposed method can be extended to arbitrary Hamiltonians, but to focus on the essentials of the proposed approach, this approximation is appropriate. In accordance with the Hamiltonian (2), the Liouville Operator $\mathcal{L}$ can be derived as [4], [20]

$$\mathcal{L} = \frac{1}{\imath\hbar}\left[\frac{\hbar^2}{2m}\left(\partial_{x'}^2 - \partial_x^2\right) + e\left(V(x) - V^\dagger(x')\right)\right]. \tag{3}$$

Utilizing the coordinate transformation

$$x = r + \frac{1}{2}q \quad \text{and} \quad x' = r - \frac{1}{2}q, \tag{4}$$

which is part of the Wigner Weyl transformation, the Liouville Operator results in

$$\mathcal{L} = \imath\frac{\hbar}{m}\partial_r\partial_q - \imath\frac{e}{\hbar}B(r,q), \tag{5}$$

in which the function $B(r,q)$ is defined by $B(r,q) = V(r + \frac{1}{2}q) - V^\dagger(r - \frac{1}{2}q)$ for the terms regarding the spatial dependence of the potential. Hence, this expression is assigned to the drift effect. The part of the Liouville Operator including the spatial derivatives can be allocated to the diffusion process.

Beyond, the application of a Fourier transform with respect to the coordinate q leads to the conventional WTE in phase space [8]. This relationship is particularly beneficial, when the quantum statistical distribution function at the boundaries has to be considered [20]. In the following, the density matrix $\rho(r + \frac{1}{2}q, r - \frac{1}{2}q, t)$ in the rotated coordinate system is addressed by the density matrix $\hat{\rho}(r,q,t)$ for simplicity.

III. Numerical Approximation Theory

The numerical approximation of the QLE according to (1) with the Liouville Operator (5) is presented following the idea of [13] for the stationary case. To start with, the computational domain defined in the interval $[-L_q/2, +L_q/2]$ with respect to the q-direction is divided into N_q cells, while the r-direction remains continuous for the moment. Taking into account a standard finite volume scheme, the integration for the QLE is carried out with respect to the i-th cell. For clarity, all integrations are performed separately.

The application of the classical midpoint rule onto the transient term leads to

$$\int_{q_{i-\frac{1}{2}}}^{q_{i+\frac{1}{2}}} dq\ \partial_t\hat{\rho}(r,q,t) \approx \Delta q_i \partial_t \hat{\rho}_i(r,t), \tag{6}$$

where the constant Δq_i represents the volume of the i-th cell. Because of this, the function $\hat{\rho}_i(r,t)$ is the cell average of the statistical density matrix. Exploiting the principal of differential and integral calculation, the term regarding the diffusion effects can be written explicitly as

$$\imath\frac{\hbar}{m}\int_{q_{i-\frac{1}{2}}}^{q_{i+\frac{1}{2}}} dq\ \partial_r\partial_q\hat{\rho} = \imath\frac{\hbar}{m}\cdot\partial_r\left[\hat{\rho}_{i+\frac{1}{2}}(r,t) - \hat{\rho}_{i-\frac{1}{2}}(r,t)\right] \tag{7}$$

with the functions $\hat{\rho}_{i\pm\frac{1}{2}}(r,t)$ being the values at the i-th cell interface. In the same manner, the integration concerning the drift effect is carried out applying the trapezoidale rule according to

$$\imath\frac{e}{\hbar}\int_{q_{i-\frac{1}{2}}}^{q_{i+\frac{1}{2}}} dq\ B(r,q)\hat{\rho}(r,q,t) \approx$$
$$\imath\frac{e}{\hbar}\Delta q_i\cdot\frac{1}{2}\left[B(r,q_{i+\frac{1}{2}})\hat{\rho}_{i+\frac{1}{2}}(r,t) + B(r,q_{i-\frac{1}{2}})\hat{\rho}_{i-\frac{1}{2}}(r,t)\right]. \tag{8}$$

The numerical values of the density matrix $\hat{\rho}_{i\pm\frac{1}{2}}(r,t)$ at the vertices of the i-th cell are approximated with the cell average of the neighbored cells

$$\hat{\rho}_{i\pm\frac{1}{2}}(r,t) = \frac{1}{2}\cdot\left[\hat{\rho}_{i\pm1}(r,t) + \hat{\rho}_i(r,t)\right]. \tag{9}$$

Along with this approximation of the cell interface values, coherent effects can be preserved within the q-direction. Under consideration of (9) the discretized equations (6), (7) and (8)

can be replaced by a matrix-vector product containing the dependence of the computational domain within the discretized q-direction with $i \in 1, \ldots, N_q$. By introducing the $N_q \times N_q$ matrices $[\Delta q]$, $[A]$ and $[C(r)]$, the QLE results in

$$[\Delta q] \cdot \partial_t \vec{\tilde{\rho}}(r,t) = \imath \frac{\hbar}{m}[A] \cdot \partial_r \vec{\tilde{\rho}}(r,t) - \imath \frac{e}{\hbar}[C(r)] \cdot \vec{\tilde{\rho}}(r,t), \tag{10}$$

where the diagonal matrix $[\Delta q]$ contains the volume Δq_i as the i-th element on the diagonal. The vector $\vec{\tilde{\rho}}(r,t)$ contains the set of averaged cell values within the q-direction. Both, the matrix $[A]$ and the matrix $[C(r)]$ are tridiagonal with non-zero contributions according to

$$A_{i,i} = 0, \quad A_{i,i+1} = +\frac{1}{2}, \quad A_{i,i-1} = -\frac{1}{2} \tag{11}$$

and

$$\begin{aligned} C_{i,i-1}(r) &= \frac{\Delta q_i}{4} \cdot B(r, q_{i-\frac{1}{2}}) \\ C_{i,i}(r) &= \frac{\Delta q_i}{4} \cdot \left[B(r, q_{i+\frac{1}{2}}) + B(r, q_{i-\frac{1}{2}}) \right] \\ C_{i,i+1}(r) &= \frac{\Delta q_i}{4} \cdot B(r, q_{i+\frac{1}{2}}). \end{aligned} \tag{12}$$

A. Introduction of a Complex Drift Operator

So far, no assumptions regarding the boundary values with respect to the q-direction have been done. Preserving the non-local character of quantum mechanics, it is evident to introduce open boundary conditions related to the so called self-energy term. However, the application of self-energies is not addressed proper until today in the field of quantum transport equations based on the QLE. Rather the assumption is made, that the boundary values can be modelled utilizing Dirichlet boundary conditions [3]–[5], [7], [20] and [21] at which the statistical density matrix has zero values corresponding to

$$\hat{\rho}(r, q = -L_q/2, t) = 0 \rightarrow \hat{\rho}_0(r,t) = 0 \tag{13}$$

and

$$\hat{\rho}(r, q = +L_q/2, t) = 0 \rightarrow \hat{\rho}_{N_q+1}(r,t) = 0. \tag{14}$$

Therefore, the system is spatially closed, whereas a spatially open behavior is desired. Consequently, the solution, especially in the non-equilibrium case, can inherently suffer under reflections from the boundaries in the q-direction.

Following the idea of self-energies, the exterior values of the discretized statistical density matrix are expressed dependent on the interior values of the statistical density matrix [13]. Unfortunately, in comparison to the Green's function or the Schrödinger formalism, there is no approach for an energy and angle dependent inclusion of self-energy terms within the rotated coordinate system. The formulation of self-energy terms within in the transformed coordinate system is beyond the scope of this work and may be a topic for future investigations.

Nevertheless, addressing the aspect of the non-physical reflections, a complex absorbing potential, which is originally used to solve the Schrödinger equation [17], [18], is utilized

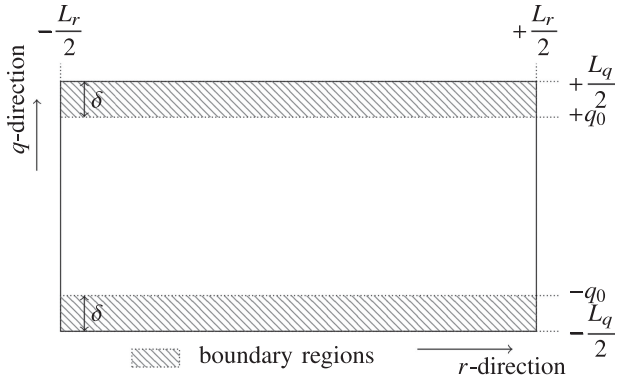

Fig. 1. Schematic diagramm of the computational domain including the boundary regions (shaded region).

to develop a new approach to overcome the limitations of the conventional boundary conditions of the QLE. For this purpose, the computational domain is extended with layers, in which the carriers exhibit a finite lifetime. These layers exhibit a width of δ with respect to the q-direction within the intervals $[-L_q/2, -q_0]$ and $[+q_0, +L_q/2]$ as depicted in Fig. 1. In the same manner as for the CAP for the Schrödinger equation, the statistical density matrix should decay in these boundary regions to a negligible value close to zero near the boundaries at $q = \pm L_q/2$. As a consequence, the Dirichlet boundary conditions at $q = \pm L_q/2$ can be applied without affecting the statistical density matrix within the interior computational domain leading to a spatially open system behavior.

For this purpose, the drift operator has to be defined in a way such that the characteristics of the CAP are retained as discussed in the following. The symmetry properties of the imaginary part of the drift operator with regard to the CAP and within the rotated coordinate system have to be taken into account. The corresponding imaginary part of the drift operator is an even function with respect to the q-direction presuming that the symmetry properties of the imaginary part of the drift operator $B(r,q)$ are given by $\Im\{B(r,q)\} = \Im\{B(r,-q)\}$. The imaginary part of the drift operator can be defined by a polynomial basis dependent on the q-direction according to $\Im\{B(r,q)\} = W(q)$. Because of the symmetry properties of $W(q)$, the expansion in the polynomial basis contains only even exponents. To avoid reflections from the layer resulting in a non-physical interference pattern within the statistical density matrix, $W(q)$ must be continuous at $q = \pm q_0$. Due to this fact, the zeroth expansion coeffiecient related to the term q^0 is equal to zero. The next simple structured approximants correspond to a set of even polynomials with the expansion coefficients W_0/δ^{2n}. Along with this approximation, the imaginary part of the drift operator $W(q)$ can be defined as

$$W(q) = \begin{cases} W_0 \cdot \dfrac{(q-q_0)^{2n}}{\delta^{2n}}, & \text{if } q_0 \le q \le q_0 + \delta \\ W_0 \cdot \dfrac{(q+q_0)^{2n}}{\delta^{2n}}, & \text{if } -q_0 - \delta \le q \le -q_0 \\ 0, & \text{elsewhere} \end{cases}, \tag{15}$$

where the constant q_0 is given by $q_0 = L_q/2 - \delta$ and n represents a natural number. The investigation of higher order approximants and their expansion coefficients within the rotated coordinate system is beyond the scope of the work. Consequently, a suitable combination of the parameters W_0 and δ has to be defined, such that a negligible reflection results. Along with these definitions, the application of the new approach leads to an appropriate description of the interior device physics as when using the CAP. In addition, this new concept can in the same manner be applied onto other quantum transport equations, i.e., the WTE. The effectiveness of this concept is discussed in Section IV.

B. Introduction of the Inflow Boundary Conditions

Addressing the boundary conditions within the r-direction, the concept of the inflow boundary condition scheme is taken up [20]. These expressions are based on the eigenvalues of the diffusion operator, a transformation onto the principal axis has to be applied [7], [13]. Hence, a transformation matrix $[\Phi]$ containing the eigenvectors $\vec{\Phi}_i$ rowwise is introduced. The application of the transformation matrix according to

$$[\Phi]^{-1}[A][\Phi] = [\lambda], \tag{16}$$

diagonalizes the matrix $[A]$. As a consequence, the matrix $[\lambda]$ includes the corresponding eigenvalues λ_i as the entries on the diagonal. The matrix $[A]$ represents a skew-symmetric, tridiagonal Toeplitz matrix with constant entries. For this case the elements $\Phi_{j,i}$ of the transformation matrix $[\Phi]$ as well as the eigenvalues λ_i can be determined analytically [22]

$$\lambda_i = \imath \cos\left(\frac{\pi \cdot i}{N_q + 1}\right) \tag{17}$$

and

$$\Phi_{j,i} = \imath^j \sin\left(\frac{j \cdot \pi \cdot i}{N_q + 1}\right) \tag{18}$$

with the indices $i, j \in 1, \ldots, N_q$. Hence, the symmetric spectrum of the matrix $[A]$ contains only imaginary values within the interval of $\lambda_i \in [-\imath, +\imath]$. Based on the sign of the imaginary part of the eigenvalue $\Im\{\lambda_i\}$ the flow characteristic is defined, in which the positive imaginary parts are identified with the forward traveling waves and negative imaginary parts are identified with the backward traveling waves, respectively, when a constant potential distribution is considered, as it is the case for the reservoir. Investigating the distribution of the eigenvalues, the value zero corresponding to bounded states is included for the case when the number of cells N_q represents an odd number. As a consequence, the resulting matrix is singular [23] reflecting the non-uniqueness of the solution when bounded states are taken into account. Obtaining uniqueness of the solution, the bounded states are excluded by applying an even number of cells N_q, only [23].

Based on the eigenvectors of the diffusion matrix, the discretized statistical density matrix can be expanded

$$\vec{\rho}(r,t) = \sum_{i=1}^{N_q} w_i(r,t) \cdot \vec{\Phi}_i = [\Phi] \cdot \vec{w}(r,t) \tag{19}$$

with the vector $\vec{w}(r,t)$ representing the set of expansion coefficients $w_i(r,t)$. Accordingly, the discretized QLE (10) can be transformed onto the principal axis leading to

$$[\Delta q] \cdot \partial_t \vec{w}(r,t) = \imath \frac{\hbar}{m}[\lambda] \cdot \partial_r \vec{w}(r,t) - \imath \frac{e}{\hbar}[G(r)] \cdot \vec{w}(r,t), \tag{20}$$

where the function $[G(r)] = [\Phi]^{-1}[C(r)][\Phi]$ is introduced.

Next, the r-direction is discretized. To start with, the interval $[-L_r/2, +L_r/2]$ with respect to the r-direction as depicted in Fig. 1 is divided into N_r cells leading to $N_r + 1$ interfaces. The application of the trapezoidale rule onto the r-direction following Heun's method leads to an ordinary system of differential equations for each cell i according to

$$\begin{aligned}
&[\Delta q]\, \frac{d}{dt}\left(\frac{\vec{w}(r_i + \Delta r_i, t) + \vec{w}(r_i, t)}{2}\right) \\
&= \imath \frac{\hbar}{m}[\lambda] \frac{\vec{w}(r_i + \Delta r_i, t) - \vec{w}(r_i)}{\Delta r_i} - \imath \frac{e}{\hbar} \\
&\quad \times \left(\frac{[G(r_i + \Delta r_i)] \cdot \vec{w}(r_i + \Delta r_i, t) + [G(r_i)] \cdot \vec{w}(r_i, t)}{2}\right),
\end{aligned} \tag{21}$$

where the parameter Δr_i represents the step width of the i-th cell with respect to the r-direction. By introducing the matrices $[T]_i, [F]_i$ and $[E]$ according to

$$[T]_i = \imath \left[\frac{\hbar}{m \cdot \Delta r_i} \cdot [\lambda] - \frac{e}{2\hbar} \cdot [G(r_i + \Delta r_i)]\right], \tag{22}$$

$$[F]_i = \imath \left[\frac{\hbar}{m \cdot \Delta r_i} \cdot [\lambda] + \frac{e}{2\hbar} \cdot [G(r_i)]\right] \tag{23}$$

and

$$[E] = \frac{1}{2}[\Delta q] \tag{24}$$

(21) can be rewritten as

$$\begin{aligned}
&[E]\, \frac{d}{dt}\left(\vec{w}(r_i + \Delta r_i, t) + \vec{w}(r_i, t)\right) \\
&= [T]_i \cdot \vec{w}(r_i + \Delta r_i, t) - [F]_i \cdot \vec{w}(r_i, t).
\end{aligned} \tag{25}$$

The system of ordinary differential equations (25) containing the discretized q-direction for each location r_i are summarized

with $i \in 1, \ldots, N_r$, resulting in a single matrix-vector equation

$$\begin{bmatrix} [E] & [E] & & & \\ & [E] & [E] & & \\ & & \ddots & \ddots & \\ & & & [E] & [E] \end{bmatrix} \cdot \frac{d}{dt}\vec{\Psi}(t) = \begin{bmatrix} -[F]_1 & +[T]_1 & & & \\ & -[F]_2 & +[T]_2 & & \\ & & \ddots & \ddots & \\ & & & -[F]_{N_r} & +[T]_{N_r} \end{bmatrix} \cdot \vec{\Psi}(t), \quad (26)$$

where the supervector $\vec{\Psi}(t)$ includes the set of the vectorial-valued expansion coefficients $\vec{w}(r_i, t)$ according to

$$\vec{\Psi}^T(t) = \left(\vec{w}(r_1, t)^T, \vec{w}(r_2, t)^T, \ldots, \vec{w}(r_{N_r}, t)^T\right). \quad (27)$$

Analyzing both system matrices, the matrix dimensions of $N_q N_r \times N_q(N_r + 1)$ can be determined. With regard to the inflow and outflow characteristics at the boundaries in the reservoirs at the discrete location $r_1 = -L_r/2$ and $r_{N_r} = +L_r/2$, the submatrices are subdivided as

$$[F]_1 = \left[[F]_1^+, [F]_1^-\right], \quad [T]_{N_r} = \left[[T]_{N_r}^+, [T]_{N_r}^-\right]$$
$$\text{and} \quad [E] = \left[[E]^+, [E]^-\right], \quad (28)$$

where the indices $^+$ and $^-$ indicate forward and backward traveling waves corresponding to either the ouflowing waves or the inflowing waves [7], [13], respectively. As discussed, the matrix $[A]$ shows a symmetric eigenvalue distribution apparent in the diagonal matrix $[\lambda]$. Hence, it can be concluded, that the subdivision results in matrices spanning a dimension of $N_q \times N_q/2$ defining the flow behavior in the reservoir. Along with this procedures the algebraic differential equation with respect to the time can be reformulated

$$\begin{bmatrix} [E]^- & [E] & & & \\ & [E] & [E] & & \\ & & \ddots & \ddots & \\ & & & [E] & [E]^+ \end{bmatrix} \cdot \frac{d}{dt}\vec{\Psi}(t) + \vec{b}_1(t) = \begin{bmatrix} -[F]_1^- & +[T]_1 & & & \\ & -[F]_2 & +[T]_2 & & \\ & & \ddots & \ddots & \\ & & & -[F]_{N_r} & +[T]_{N_r}^+ \end{bmatrix} \cdot \vec{\Psi}(t) + \vec{b}_2(t) \quad (29)$$

with the boundary vectors $\vec{b}_1(t)$ and $\vec{b}_2(t)$ containing the inflow characteristics

$$\vec{b}_1(t) = \begin{pmatrix} [E]^+ \frac{d}{dt}\vec{\Psi}(r_1, \lambda > 0, t) \\ 0 \\ \vdots \\ 0 \\ [E]^- \frac{d}{dt}\vec{\Psi}(r_{N_r}, \lambda < 0, t) \end{pmatrix} \quad (30)$$

and

$$\vec{b}_2(t) = \begin{pmatrix} -[F]_1^+ \vec{\Psi}(r_1, \lambda > 0, t) \\ 0 \\ \vdots \\ 0 \\ [T]_{N_r}^- \vec{\Psi}(r_{N_r}, \lambda < 0, t) \end{pmatrix}. \quad (31)$$

Now, the reduced system matrices span a quadratic dimension with $N_r N_q \times N_r N_q$. Including the inflow characteristics, the boundary vectors $\vec{b}_1(t)$ and $\vec{b}_2(t)$ contain the quantum statistical distribution function. In contrast to the standard UDS [3]–[5], [21], the boundary condition is not only related to the diffusion process, rather the boundary condition is in addition inherently linked with the potential distribution [7] as can be observed from the matrices $[F]_1^+$ and $[T]_{N_R}^-$ in (22) and (23).

An appropriate quantum statistical distribution function can be defined in the phase space in dependence of the variable k represented by the Fermi-Dirac statistics [20]

$$f(k) = \frac{m k_B T}{2\pi\hbar^2} \cdot \ln\left\{1 + \exp\left[-\frac{1}{k_B T} \cdot \left(\frac{\hbar^2 k^2}{2m} - \mu\right)\right]\right\}, \quad (32)$$

where the parameter μ represents the chemical potential. The constant k_B is the Boltzmann constant and the variable T is the absolute temperature. According to the thermodynamic equilibrium within the reservoir, the chemical potential μ is calculated in dependence of the doping concentration N_d and the absolute temperature T utilizing the equilibrium of the charge carriers. The application of the inverse Fourier transformation with respect to the phase space variable k results in the real space representation $\hat{f}(q)$ of the Fermi-Dirac distribution function

$$\hat{f}(q) = \frac{1}{2\pi}\int dk \, \cos(q \cdot k) \cdot f(k) \quad (33)$$

exploiting the fact that the function $f(k)$ is even. Based on the eigenvectors of the diffusion matrix (18), the discretized quantum statistical distribution function $\vec{\hat{f}}$ at the boundaries of the computational domain at r_1 and r_{N_r} can be expanded

$$\vec{\hat{f}} = \sum_{i=1}^{N_q} \psi_i \cdot \vec{\Phi}_i = [\Phi] \cdot \vec{\psi}, \quad (34)$$

where the vector $\vec{\psi}$ with the dimension $N_q \times 1$ represents the set of expansion coefficients ψ_i related to the corresponding

eigenvector Φ_i and eigenvalue λ_i. The discretized distribution function $\vec{\psi}$ can be separated with regard to the inflow behavior related to the vectors $\vec{\psi}_{\mathrm{p}}$ and $\vec{\psi}_{\mathrm{n}}$ spanning a dimension of $N_q/2 \times 1$

$$\begin{aligned} \vec{\psi}_{\mathrm{p}} &= \vec{\psi}, \quad \text{where } \Im\{\lambda\} > 0 \\ \vec{\psi}_{\mathrm{n}} &= \vec{\psi}, \quad \text{where } \Im\{\lambda\} < 0. \end{aligned} \tag{35}$$

As long as the inflow behavior of the device can be assumed to be time independent, the boundary vector $\vec{b}_1(t)$ represents a zero-valued function. However, utilizing the equations (35) the inflow boundary vector $\vec{b}_2(t)$ is given by

$$\vec{b}_2(t) = \vec{b}_2 = \begin{pmatrix} -[F]_1^+ \, \vec{\psi}_{\mathrm{p}} \\ 0 \\ \vdots \\ 0 \\ [T]_{N_r}^- \, \vec{\psi}_{\mathrm{n}} \end{pmatrix}, \tag{36}$$

where the inflow behavior is assumed to be time independent. For the investigation of the stationary regime, the transient part of the equation (29) corresponding to the left hand side has to be neglected resulting in the matrix-vector equation

$$\begin{bmatrix} -[F]_1^- & +[T]_1 & & & \\ & -[F]_2 & +[T]_2 & & \\ & & \ddots & \ddots & \\ & & & -[F]_{N_r} & +[T]_{N_r}^+ \end{bmatrix} \cdot \vec{\Psi}_{\mathrm{inf}} = -\vec{b}_2, \tag{37}$$

where the vector $\vec{\Psi}_{\mathrm{inf}}$ represents the stationary solution vector. The discretized real space presentation of the statistical density matrix can be obtained by the application of the transformation matrix (19). Beyond, this system of equations for the stationary regime is equivalent to the first order Taylor approximation of the expotential operator [13], which is in accordance with the results obtained from the QTBM [14] in the self-consistent non-equilibrium case. The solution of the stationary regime $\vec{\Psi}_{\mathrm{inf}}$ may represent an appropriate initial condition at the time $t = 0$ for the transient regime. Furthermore, the solution $\vec{\Psi}_{\mathrm{inf}}$ also provides a detailed insight of the stationary behavior of the statistical density matrix and can therefore also be used for comparison with the steady state density matrix obtained from the transient calculations $\vec{\Psi}(t \to \infty)$. For the solution of the transient QLE conventional implicit schemes [24] such as the Crank-Nicolson scheme and explicit schemes [25], [26] as the Runge-Kutta schemes can be applied. In practice, the application of implicit schemes can cause difficulties as on the one hand the inversion of the system matrix is combined with high computational costs. On the other hand, the Hartree-Fock-potential represents a time-dependent function in the transient regime. In this approach we consider the flat band model for presentation purposes. Of course, the presented method can be extended to the self-consistent case. Then, the approximation of the Hartree-Fock-potential for the next time step has to be resolved.

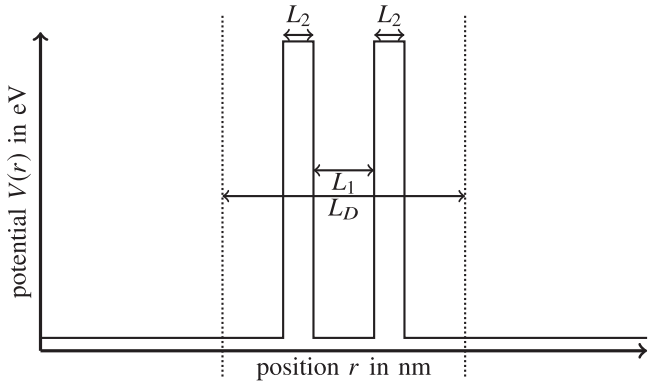

Fig. 2. Schematic diagramm of the potential distribution $V(r)$ for the case of the resonant tunneling diode with the parameters defined in the text.

IV. Numerical Results and Discussion

For the evaluation of the proposed approach, a standard resonant tunneling diode based on the material system GaAs/AlGaAs is taken up allowing a straightforward comparison with other methods as depicted in Fig. 2. The computational domain exhibits a length of $L_r = 106$ nm with respect to the r-direction.

The spatially varying portion of the potential distribution takes place within the region of $L_D = 30$ nm. Symmetrically ordered to the origin, the $\mathrm{Al}_{0.21}\mathrm{GaAs}_{0.79}$-barriers have a width of $L_2 = 5$ nm enclosing the $L_1 = 6$ nm wide quantum well. Furthermore, the energy value of the material GaAs is defined as the energy reference value leading to a maximum potential value of 0.1768 eV within the AlGaAs-barriers. The length of the device within the q-direction is set to $L_q = 152$ nm. For the discretization in r-direction $N_r = 167$ cells and in q-direction $N_q = 180$ cells are used, respectively. Avoiding reflections from the boundary with regard to the q-direction, the parameters of the imaginary part of the drift operator (15) are set to a length of $\delta = 0.2 \cdot L_q$, $W_0 = 1$ eV and $n = 1$.

A. Impact of the Complex Drift Operator

The requirement of a complex drift operator including $W(q)$ is discussed in the following. For presentation purposes we compare the imaginary parts of the density matrices $\Im\{\hat{\rho}(r, q, t)\}$ as reflections dominantly affect the imaginary part of the statistical density matrix in contrast to their real parts. As initial statistical density matrix, the steady state equilibrium statistical density matrix obtained from the numerical solution of equation (37) is taken for $t = 0$. Then, the resonant tunneling device is driven out of equilibrium by applying a constant applied bias of $U = -0.77$ V for $t > 0$.

For the approximation of the discretized QLE (29) in the time domain, a computational efficient Low Storage Runge Kutta scheme (LSRK) of fourth order is used [26]. As the Runge Kutta scheme is an explicit scheme, a time step of $\Delta t = 0.02$ fs is applied to obtain stable results. The statistical density matrix is calculated iteratively from the equilibrium state to $t = 250$ fs for both cases, applying conventional boundary conditions and applying the complex drift operator. The imaginary part of the statistical density matrix after $t = 250$ fs is depicted in Fig. 3(a)

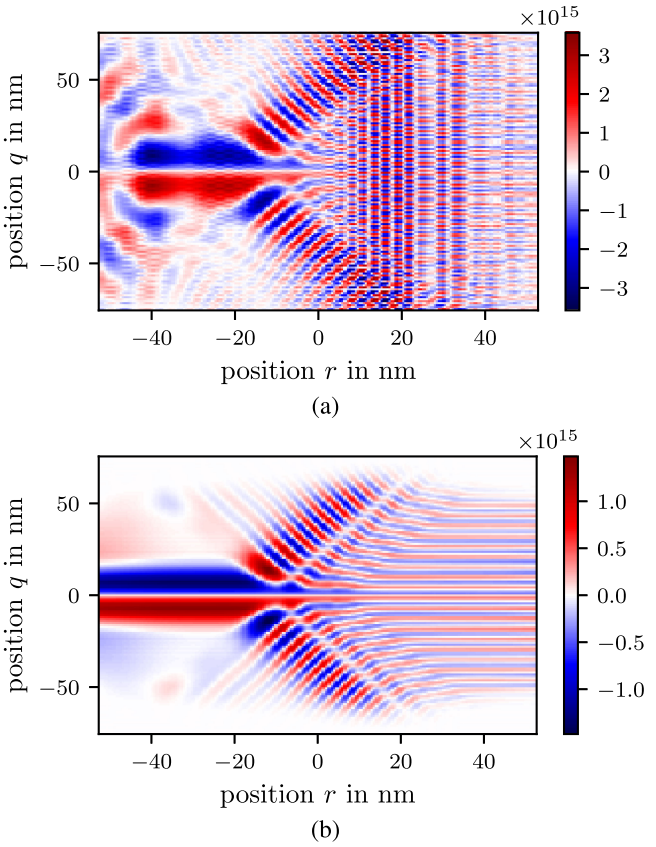

Fig. 3. (a) Imaginary part of the density matrix $\Im\{\hat{\rho}(r,q,t)\}$ after $t = 250$ fs applying the conventional boundary conditions and (b) the complex drift operator considering the case of the resonant tunneling diode with an external applied bias of $U = -0.77$ V.

applying only the conventional Dirichlet boundary conditions with respect to the q-direction. Additionally, including the concept of the complex drift operator, the imaginary part of the statistical density matrix after $t = 250$ fs is depicted in Fig. 3(b). The comparison of the statistical density matrices allows the observation of a highly oscillating interference pattern in Fig. 3(a) utilizing conventional boundary conditions, only. In contrast, the numerical solution applying the complex drift operator circumvents these non-physical reflections caused by the boundaries as shown in Fig. 3(b). Therefore, regarding the open boundary conditions related to the self energy terms, the behavior at the boundaries with respect to the q-direction is not properly addressed without the concept of the complex drift operator. Consequently, non-physical results are obtained as depicted in Fig. 3(a). In particular, the imaginary part of the density matrix is related to the current density according to

$$j(r,t) = \frac{\hbar}{m}\Im\left\{\partial_q\ \hat{\rho}(r,q,t)|_{q=0}\right\}. \tag{38}$$

Hence, the interference pattern can cause a non-physical spatially varying current density within the ballistic regime applying only conventional boundary conditions. Additionally, the real part of the density matrix can be allocated to the carrier density

$$n(r,t) = \Re\left\{\hat{\rho}(r,q,t)\,|_{q=0}\right\} \tag{39}$$

suffering from the interference pattern as well.

With regard to engineering applications, the complex drift operator rendering the open boundary conditions in the q-direction, is preferable in this approach as explained in the following. As defined in the concept of the self-energies, the exterior values of the density matrix are expressed in dependence of the interior values of the density matrix with respect to the q-direction leading to additional entries in the drift matrix and the diffusion matrix [13]. The statistical density matrix represents a function dependent on both space coordinates, r and q. Therefore, the interaction of the exterior with the interior statistical denstiy matrix with respect to the q-direction can differ at each location r. As a result the self-energy term with respect to the q-direction can differ at each location r. Accordingly, the additional entries in the diffusion matrix $[A]$ in (10), which embody the self-energy terms, cause a dependence of the r-direction in the diffusion matrix $[A]$ as well. Hence, the eigenvalues and eigenvectors of the diffusion matrix $[A]$ in (16) defining the inflow and outflow behavior have to be calculated for each discretized location r_i. In summary, the evaluation of the density matrix can be computational costly applying the concept of self-energy terms. Beyond that, the commutator consisting of the spatial derivative with respect to the r-direction and the self-energy terms being a function dependent on the r-direction would have been to be considered for an adequate inclusion of the diffusion process.

In contrast, the new approach represents only a modification concerning the drift matrix. Therefore, the above mentioned drawbacks can be effectively circumvented.

B. Transient Evolution of the Carrier Density

To demonstrate the advantages of the proposed method, a comparison with the conventional numerical methods solving the WTE based on a second order UDS [21] is presented. Until today, the UDS is the state of art computational technique with regard to the solution of the WTE, although the numerical solution is associtated with some serious problems [7], [12], [13]. Especially, the coherent effects cannot obeyed by utilizing the UDS leading to an overestimation of the diffusion process. As a consequence non-physical results can be obtained [7], [12], [13].

As initial statistical density matrix, the steady state equilibrium density matrix is taken at $t = 0$ fs. Then, an external bias of $U = -0.27$ V is applied to the device driving the density matrix into the transient non equilibrium state. For both methods, a LSRK of fourth order [26] is used for the approximation of the time derivative with a time step according to $\Delta t = 0.02$ fs. The iteratively calculated carrier densities obtained from the proposed approach and the numerical solution of the WTE applying the second order UDS are depicted in Fig. 4 for different time steps. To start with, the initial carrier densities at $t = 0$ fs are compared. Tracing back to the overestimation of the diffusion process, the carrier density is remarkable lower for the case of the WTE between the barriers forming the resonant

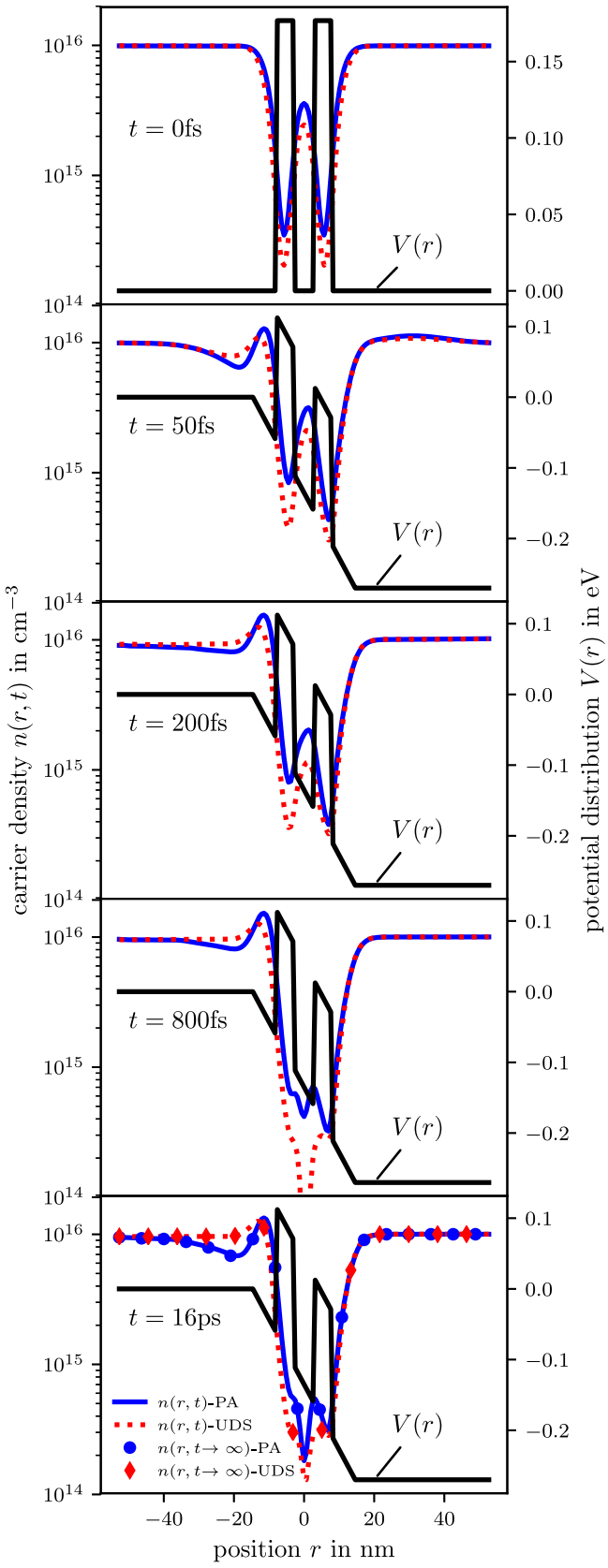

Fig. 4. Carrier densities $n(r,t)$ for the case of the conventional second order UDS (dotted) and the proposed approach (PA) (solid) considering a resonant tunneling diode with the corresponding potential distribution $V(r)$.

structure. Furthermore, a non-physical oscillation pattern located in the reservoirs can be observed in the carrier density for the case of the WTE. As the point hereby is discussed in [7], [13], the oscillation pattern is not shown here. After $t = 800$ fs a non-physical result is obtained for the case of the WTE observing negative values of the carrier density within the quantum well region. Due to the intention of a clear presentation on a logarithmic scale, these values cannot be depicted here. Along with the proposed approach only physical results can be obtained. Both methods converge towards the corresponding stationary steady state solution $n(r, t \to \infty)$ for the applied bias as shown in Fig. 4. The carrier density for the case of the proposed approach reaches the steady state solution after approximate 15 ps, while the carrier density for the case of the WTE utilizing the conventional second order UDS reaches the steady state after approximate 1 ps. This same deviation in the results can be observed and confirmed for different dense resolutions of the computational domain, ensuring a numerical convergence of the results. Due to this fact, the deviation can only be a result of the different methodologies. In comparison to the proposed approach, the UDS cannot describe the coherent effects adequately [7], [13]. Particularly, in the front of the left AlGaAs barrier this effect is dominant. In this region a maximum accumulation of carriers at approximately 2.5 ps can be observed. Then, this accumulation is depleted resulting in the steady state solution at about 15 ps. The carrier density within the quantum well and within the region beyond the right AlGaAs barrier reaches the steady state at nearly 1.5 ps. An adequate description of the coherent effects is a prerequisite with regard to high frequency applications.

The non-physical results, which can be a consequence of the inappropriate inclusion of the coherent effects, can be circumvented in comparison to the standard UDS. Furthermore, the proposed approach converges exactly towards the steady state solution as can be observed from Fig. 4. As already mentioned, the stationary solution of the proposed approach (37) is mathematically equivalent with the first order Taylor approximation of the exponential operator approach in [13], which is in accordance with the results obtained from the QTBM [14]. Therefore, it can be concluded, that the transient scheme converges towards the correct physical solution.

V. Summary and Conclusion

A novel numerical solution technique for the transient analysis of the Quantum Liouville Equation has been presented, justified and discussed. To address the issue of open boundary conditions with respect to the q-direction, a complex drift operator is defined. The proposed approach inherently includes an adequate description of coherent effects, so that unphysical results can be circumvented. Additionally, the time dependency of the quantum statistical distribution function can be considered, allowing the description of non-local processes within the time domain, which can be investigated in the future.

REFERENCES

[1] R. Lake and S. Datta, "Nonequilibrium Green's function method applied to double-barrier resonant-tunneling diodes," *Phys. Rev. B*, vol. 45, no. 12, pp. 6670–6685, 1992.

[2] A. P. Jauho, N. S. Green, and Y. Meir, "Time-dependent transport in interacting and noninteracting resonant-tunneling systems," *Phys. Rev. B*, vol. 50, no. 8, pp. 5528–5544, 1994.

[3] W. R. Frensley, "Quantum transport modeling of resonant tunneling devices," *Solid-State Electron.*, vol. 31, no. 3/4, pp. 739–742, 1988.

[4] W. R. Frensley, "Wigner-function model of a resonant-tunneling semiconductor device," *Phys. Rev. B* vol. 36, no. 3, pp. 1570–1580, 1987.

[5] W. R. Frensley, "Transient response of a tunneling device obtained from the wigner function," *Phys. Rev. Lett.*, vol. 57, no. 22, pp. 2853–2856, 1986.

[6] F. Rossi, C. Jacoboni, and M. Nedjalkov, "A monte carlo solution of the wigner transport equation," *Semicond. Sci. Technol.*, vol. 9, no. 5S, pp. 934–936, 1994.

[7] D. Schulz and A. Mahmood, "Approximation of a phase space operator for the numerical solution of the Wigner transport equation," *IEEE J. Quantum Electron.*, vol. 52, no. 2, Feb. 2016, Art. no. 8700109.

[8] E. Wigner, "On the quantum correction for thermodynamic equilibrium," *Phys. Rev.*, vol. 40, pp. 749–759, 1932.

[9] F. Dolcini, R. C. Iotti, and F. Rossi, "Interplay between energy dissipation and reservoir-induced thermalization in nonequilibrium quantum nanodevices," *Phys. Rev. B*, vol. 88, no. 11, 2013, Art. no. 115421.

[10] R. Rosati, R. C. Iotti, F. Dolcini, and F. Rossi, "Derivation of nonlinear single-particle equations via many-body Lindblad superoperators: A density-matrix approach," *Phys. Rev. B*, vol. 90, no. 12, 2014, Art. no. 125140.

[11] R. Courant, E. Isaacson, and M. Rees, "On the solution of nonlinear hyperbolic differential equations by finite differences," *Commun. Pure Appl. Math.*, vol. 5, no. 3, pp. 243–255, 1952.

[12] R. Rosati, F. Dolcini, R. C. Iotti, and F. Rossi, "Wigner function formalism applied to semiconductor quantum devices: Failure of the conventional boundary condition scheme," *Phys. Rev. B*, vol. 88, no. 3, pp. 3451–3466, 2013.

[13] K. S. Khalid, L. Schulz, and D. Schulz, "Self-energy concept for the numerical solution of the liouville-von neumann equation," *IEEE Trans. Nanotechnol.*, vol. 16, no. 6, pp. 1053–1061, Nov. 2017.

[14] C. S. Lent and D. J. Kirkner, "The quantum transmitting boundary method," *J. Appl. Phys.*, vol. 67, no. 10, pp. 6653–6359, 1990.

[15] H. Jiang, S. Shao, W. Cai, and P. Zhang, "Boundary treatments in nonequilibrium Greens function (NEGF) methods for quantum transport in nano-MOSFETs," *J. Comput. Phys.*, vol. 227, no. 13, pp. 6553–6573, 2008.

[16] Y. He, T. Kubis, M. Povolotskyi, J. Fonseca, and G. Klimeck, "Quantum transport in NEMO5: Algorithm improvements and high performance implementation," in *Proc. IEEE Int. Conf. Simul. Semicond. Processes Device*, 2014, pp. 361–364.

[17] U. Riss and H. Meyer, "Calculation of resonance energies and widths using the complex absorbing potential method," *J. Phys. B, At. Mol. Opt. Phys*, vol. 26, no. 23, pp. 4503–4535, 1993.

[18] D. Neuhasuer and M. Baer, "The time-dependent Schrödinger equation: Application of absorbing boundary conditions," *J. Chem. Phys.*, vol. 90, no. 8, pp. 4351–4355, 1989.

[19] H. Mizuta and C. J. Goodings, "Transient quantum transport simulation based on the statistical density matrix," *J. Phys. Condens. Matter*, vol. 3, no. 21, pp. 3739–3756, 1991.

[20] W. Frensley, "Boundary conditions for open quantum systems driven far away from equilibrium," *Rev. Mod. Phys.*, vol. 62, no. 3, pp. 741–791, 1990.

[21] K. Y. Kim and B. Lee, "Simulation of quantum transport by applying second order differencing scheme to Wigner function model including spatially varying mass," *Solid-State Electron.*, vol. 43, no. 1, pp. 81–86, 1999.

[22] S. Noschese, L. Pasquini, and L. Reichel, "Tridiagonal toeplitz matrices: Properties and novel applications," *Numer. Linear Algebra Appl.*, vol. 20, no. 2, pp. 302–326, 2013.

[23] A. Arnold, H. Lange, and P. Zweifel, "A discrete-velocity, stationary Wigner equation," *J. Math. Phys.*, vol. 41, no. 11, pp. 7167–7180, 2000.

[24] K. L. Jensen and F. A. Buot, "Numerical simulation of transient response and resonant-tunneling characteristics of double-barrier semiconductor structures as a function of experimental parameters," *J. Appl. Phys.*, vol. 65, pp. 5248–5250, 1989.

[25] A. Arnold and C. Ringhofer, "An operator splitting method for the Wigner-Poisson problem," *SIAM J. Numer. Anal.*, vol. 33, no. 4, pp. 1622–1643, 1996.

[26] J. H. Williamson, "Low-storage Runge-Kutta schemes," *J. Comput. Phys.*, vol. 35, no. 1, pp. 48–56, 1980.

Lukas Schulz was born in Recklinghausen, Germany, in 1992. He received the B.Sc. and the M.Sc. degrees in electrical engineering and information technology from Technische Universität Dortmund, Dortmund, Germany, in 2015 and 2017, respectively. He has been a Research Assistant with the Chair of High Frequency Techniques, Technische Universität Dortmund, since 2017. He is currently working on the simulation of quantum devices including coherent and kinetic models.

Dirk Schulz was born in Düsseldorf, Germany, in 1965. He received the Dipl.Ing. degree in electrical engineering from the RWTH Aachen University, Aachen, Germany, in 1990, and the Dr.Ing. and Venia Legendi degrees from the Technische Universität Dortmund, Dortmund, Germany, in 1994 and 2001, respectively. He has been a Research Assistant with the Chair of High Frequency Techniques, Technische Universität Dortmund, since 1990. He is currently working in the field of modeling and simulation of photonic and terahertz devices.